Projected Twenty-First-Century Changes in the Length of the Tropical Cyclone Season

John G. Dwyer,[*,##] Suzana J. Camargo,[+] Adam H. Sobel,[*,#,+] Michela Biasutti,[+] Kerry A. Emanuel,[@] Gabriel A. Vecchi,[&,**] Ming Zhao,[&] and Michael K. Tippett[*,++]

[*] Department of Applied Physics and Applied Mathematics, Columbia University, New York, New York
[+] Lamont-Doherty Earth Observatory, Columbia University, Palisades, New York
[#] Department of Earth and Environmental Sciences, Columbia University, New York, New York
[@] Program in Atmospheres, Oceans and Climate, Massachusetts Institute of Technology, Cambridge, Massachusetts
[&] National Oceanic and Atmospheric Administration/Geophysical Fluid Dynamics Laboratory, Princeton, New Jersey
[**] Program in Atmospheric and Oceanic Sciences, Princeton University, Princeton, New Jersey
[++] Center of Excellence for Climate Change Research, Department of Meteorology, King Abdulaziz University, Jeddah, Saudi Arabia

ABSTRACT

This study investigates projected changes in the length of the tropical cyclone season due to greenhouse gas increases. Two sets of simulations are analyzed, both of which capture the relevant features of the observed annual cycle of tropical cyclones in the recent historical record. Both sets use output from the general circulation models (GCMs) of either phase 3 or phase 5 of the CMIP suite (CMIP3 and CMIP5, respectively). In one set, downscaling is performed by randomly seeding incipient vortices into the large-scale atmospheric conditions simulated by each GCM and simulating the vortices' evolution in an axisymmetric dynamical tropical cyclone model; in the other set, the GCMs' sea surface temperature (SST) is used as the boundary condition for a high-resolution global atmospheric model (HiRAM). The downscaling model projects a longer season (in the late twenty-first century compared to the twentieth century) in most basins when using CMIP5 data but a slightly shorter season using CMIP3. HiRAM with either CMIP3 or CMIP5 SST anomalies projects a shorter tropical cyclone season in most basins. Season length is measured by the number of consecutive days that the mean cyclone count is greater than a fixed threshold, but other metrics give consistent results. The projected season length changes are also consistent with the large-scale changes, as measured by a genesis index of tropical cyclones. The season length changes are mostly explained by an idealized year-round multiplicative change in tropical cyclone frequency, but additional changes in the transition months also contribute.

1. Introduction

The active seasons for tropical cyclones (TCs) vary widely across different basins within the same hemisphere. For example, in the North Atlantic Ocean the

[##] Current affiliation: Program in Atmospheres, Oceans and Climate, Massachusetts Institute of Technology, Cambridge, Massachusetts.

Corresponding author address: John G. Dwyer, Program in Atmospheres, Oceans and Climate, Massachusetts Institute of Technology, Room 54-1823, 77 Massachusetts Avenue, Cambridge, MA 02139.
E-mail: jgdwyer@mit.edu

peak season is the late summer to early fall (August–October) with the official season defined from June to November. In the western North Pacific Ocean, TCs form throughout the year, while in the north Indian Ocean TCs mainly form before and after the monsoon season. As greenhouse gas concentrations increase and the climate warms, the lengths and durations of the tropical cyclone seasons may change. Already, observational studies have found trends toward longer TC season lengths in the North Atlantic Ocean (Kossin 2008) and South China Sea (Yan et al. 2012) in the recent historical record. Other work has shown that the timing of the TC season is sensitive to the radiative balance, so that during the mid-Holocene, the Northern Hemisphere TC annual cycle (as delineated by the large-scale environment for TC activity

in climate model simulations) shifted to later in the calendar year in response to increased boreal summer insolation (Korty et al. 2012).

Our interest in the possibility of greenhouse gas–induced changes in tropical cyclone seasonality stems from global climate model (GCM) projections of changes in the annual cycles of other climate variables in response to increasing greenhouse gases. In the tropics and subtropics, the World Climate Research Programme's (WCRP's) Coupled Model Intercomparison Project (CMIP), phase 3 (CMIP3; Meehl et al. 2007) and phase 5 (CMIP5; Taylor et al. 2012), multimodel datasets project increases in the annual ranges of temperature and precipitation as well as a shift of the annual cycles of these variables to later in the year (Chou et al. 2007; Biasutti and Sobel 2009; Sobel and Camargo 2011; Dwyer et al. 2012; Seth et al. 2013; Huang et al. 2013; Dwyer et al. 2014). Motivated by the robustness of these seasonality changes (nearly all models agree on the sign), we initially hypothesized that the timing shift and increase in the annual range of SST could be affecting the seasonality of tropical cyclones in a similar manner. Do GCMs project tropical cyclones to respond similarly to SST?

Unfortunately, coupled GCMs, including those used in CMIP5 and CMIP3, do not have sufficient horizontal resolution to accurately simulate all characteristics of tropical cyclones (especially intensity), making projections of future behavior difficult (e.g., Camargo 2013). A common alternate approach is to use less comprehensive models, which do not attempt to simulate a fully coupled atmosphere and ocean, to reproduce the observed distribution of TCs in both space and time and to provide clues as to how TCs may change in the future. This study focuses on TC projections produced by two of these methods. The first method employs a statistical–dynamical downscaling approach in which incipient vortices are seeded into large-scale conditions from a GCM and then simulated with an idealized axisymmetric dynamical tropical cyclone model, following a track determined using the GCM wind field (Emanuel et al. 2008); while the other method, a high-resolution global atmospheric model (HiRAM; Held and Zhao 2011), can explicitly, albeit crudely, resolve TCs when given the SST as a boundary condition.

Despite the advances of GCMs and new modeling approaches and techniques, uncertainty remains in projections of TC frequency with global warming. High-resolution global atmospheric models, including HiRAM, have predicted a reduction in the global number of TCs (e.g., Sugi et al. 2002; Bengtsson et al. 2007; Knutson et al. 2010). Unlike these models, the downscaling approach described above when applied to CMIP5 data (Emanuel 2013) projects an increase in the global number of storms

by the end of the twenty-first century. When that same downscaling technique is applied to the CMIP3 dataset, though, it projects a reduction in the global TC frequency in the future, in agreement with other studies (Emanuel et al. 2008). Furthermore, other CMIP5 analyses (Camargo 2013; Tory et al. 2013; Murakami et al. 2014) project a reduction of global TC frequency by the end of the twenty-first century for most models. Regional changes in TC frequency are more uncertain (e.g., Knutson et al. 2008; Villarini and Vecchi 2012, 2013; Knutson et al. 2013; Wu et al. 2014).

Here we investigate how the timing of the tropical cyclone season is projected to change due to increased greenhouse gases and other anthropogenic effects and relate these changes to changes in environmental characteristics, using both the downscaling model and HiRAM forced with CMIP3 and CMIP5 data. In the following section we describe the data and explain the methods we use. In section 3, we describe the twentieth-century seasonal cycles in HiRAM and the downscaling model and compare them with observations. In sections 4 and 5 we describe the projected changes in the length of the TC season and in a genesis index for tropical cyclones. Finally, in section 6, we summarize our findings.

2. Data and methods

We consider two sets of simulations that make use of coupled model data. The first is the statistical–dynamical downscaling method of Emanuel et al. (2006). This method randomly seeds incipient vortices into environmental conditions produced by GCMs and then simulates the further evolution of each vortex using an idealized axisymmetric dynamical tropical cyclone model. For each GCM, the number of seeds is tuned so that the annual number of tropical cyclones that form matches that of the current climate in the annual mean. The large-scale winds determine the track of the potential TC using a "beta and advection" model. The dynamical model used to compute the wind field of the storm is the Coupled Hurricane Intensity Prediction System (Emanuel et al. 2004), a deterministic, coupled air–sea model in angular momentum space. This method was used to generate the equivalent of many years of storms for any given climate scenario.

The statistical–dynamical downscaling method was previously run on the following CMIP5 models: NCAR CCSM4, GFDL CM3, HadGEM2-ES, MPI-ESM-MR, MIROC5, and MRI-CGCM3 for the twentieth-century historical simulation and the twenty-first-century representative concentration pathway 8.5 (RCP8.5) scenario as described in Emanuel (2013). We refer to these simulations collectively as D5. We calculate changes in the TC

statistics averaged over 1975–2000 in the historical simulation and 2075–2100 in the RCP8.5 simulation. We also study the TCs downscaled from the following CMIP3 models (D3) for the 20C3M and twenty-first-century SRES A1B scenarios: CCSM3, CNRM-CM3, CSIRO Mk3.0, ECHAM5, GFDL CM2.0, MIROC3.2(medres), MRI-CGCM2.3.2, and fully described in Emanuel et al. (2008). These downscaling simulations were run using coupled model output averaged over 1970–2000 and 2070–2100. (Expansions for acronyms are available at http://www.ametsoc.org/PubsAcronymList.)

The other set of simulations we analyze was produced by the High Resolution Atmospheric Model (HiRAM), an atmospheric GCM at 50-km horizontal resolution using prescribed surface boundary conditions (Held and Zhao 2011). TCs are identified and tracked using an algorithm that identifies features of maximum vorticity and minimum pressure within a warm core (Zhao et al. 2009). We study the HiRAM response to the twenty-first-century SST anomaly patterns generated by the CMIP3 and CMIP5 ensembles, compared with a control simulation run with observed, climatological SST from 1981 to 2005. The future simulations use the SST perturbation from the end of the twenty-first century in the CMIP suites added to the twentieth-century-observed SST pattern, as described in detail in Zhao et al. (2009) and Zhao and Held (2012). For CMIP5, we look at the multimodel mean SST warming in the RCP4.5 scenario (about half of the forcing strength of the RCP8.5 scenario used by the D5 models). For CMIP3, we study the response in individual A1B models (CCCma CGCM3.1, ECHAM5, GFDL CM2.1, GFDL CM2.0, HadCM3, HadGEM1, MIROC3.2, and MRI-CGCM2.3.2) as well as the response to the multimodel mean SST increase. Because each set of simulations includes different models and different forcing scenarios, a direct comparison of the results incorporates variability arising from different projections of twenty-first-century climate. We refer to HiRAM forced with the CMIP5 multimodel mean SST anomaly as H5 and HiRAM forced with CMIP3 SST anomalies as H3. The control simulation is run for 25 years, the simulation with the multimodel mean SST perturbation for 20 years, and the simulations with SST anomalies from individual CMIP3 models for 10 years. The simulation lengths and number of SST perturbations (especially for H5) are constrained by the large computational resources demanded for high-resolution modeling.

Observational TC data come from the best-track datasets of the National Hurricane Center for North and South Atlantic (NA and SA), eastern North Pacific (ENP), and central North Pacific (CNP) basins (NHC 2015; Landsea and Franklin 2013), and from the Joint
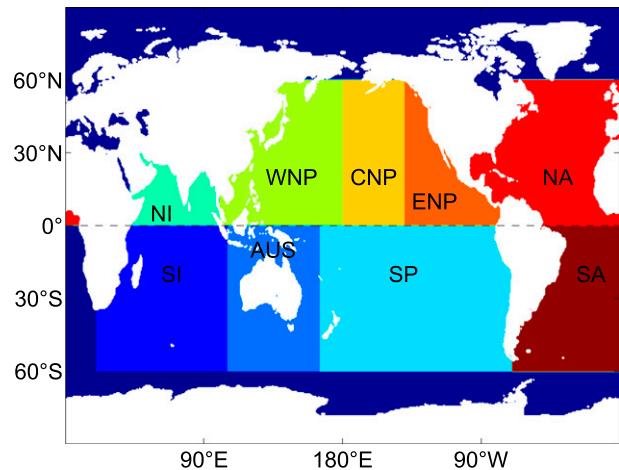
FIG. 1. Our basin definitions and abbreviations used in subsequent figures.

Typhoon Warning Center for the western North Pacific (WNP), north Indian Ocean (NI), south Indian Ocean (SI), Australian (AUS), and South Pacific (SP) basins (JTWC 2015; Chu et al. 2002). The seasonal cycle of TCs is not very sensitive to the choice of dataset (Schreck et al. 2014). To ensure an accurate representation of the seasonal cycle in all basins, we calculate the climatology only over the satellite era (1980–2012).

Basin definitions are shown in Fig. 1. TCs are only counted in their genesis basin and genesis month, unless they form in the last two days of the month and persist for more than four days, in which case they are counted in the following month. We require TC events to have a peak sustained wind speed of at least 35 kt (1 kt $\approx$ 0.51 m s^{-1}; this excludes tropical depressions from our analysis). Because TCs in D5 have been characterized at a higher threshold (40 kt), we perform a correction to account for this small discrepancy in threshold wind speed. Observations show the global average number of TCs per year is 85.1 with a 35-kt threshold and 79.1 with a 40-kt threshold, giving a ratio of 1.08. We multiply the twentieth- and twenty-first-century D5 data in each basin by this ratio to roughly account for the stricter threshold. Note that this procedure has little effect on changes in season length, but it increases the global, annual mean number of TCs identified by D5.

In previous studies of seasonality changes in other variables (Biasutti and Sobel 2009; Dwyer et al. 2012, 2014), we have performed a Fourier transform to obtain the phase and amplitude of the annual cycle. The phase indicates the timing of the annual cycle relative to the calendar year and the amplitude is a measure of the annual range. An alternative approach is to define seasonality by the length of time a variable is larger than a certain threshold value, as is often used in the biological

Monthly Climatology of Tropical Cyclone Frequency
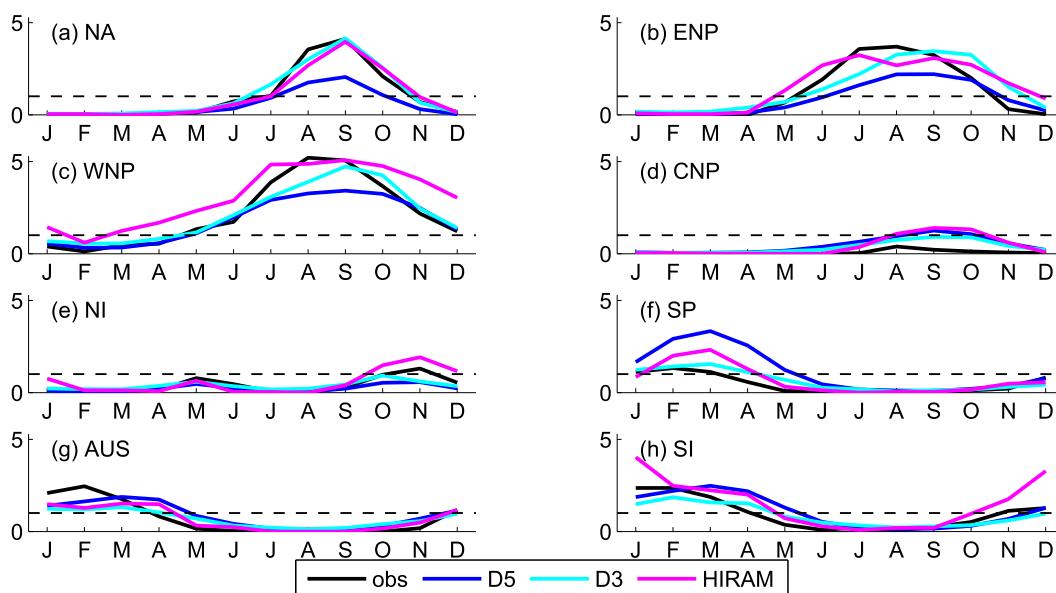
FIG. 2. Seasonal cycles of the number of TCs in different ocean basins. We plot data from observations (solid black line), the downscaled historical CMIP5 data (D5, dark blue line), the downscaled 20C3M CMIP3 data (D3, cyan line), and HiRAM forced with observed SST (magenta line). The thin dashed horizontal black line indicates a threshold of one tropical storm per month. Because D5 and D3 are run with SST from climate models, while HiRAM is run with observed SST, these simulations are not directly comparable.

and phenological literature. For surface temperature, annual mean changes lead to changes in threshold-based season lengths so directly (e.g., summer as defined by temperature above a given threshold lengthens when the climate warms) as to be almost trivial, motivating a focus on changes in the Fourier-defined seasons, since those are not as obviously expected.

In the case of tropical cyclones, though, Fourier-defined seasonality is a less natural measure than threshold-based seasonality for two reasons. One reason is that most ocean basins have no or very few TCs during the winter months, cropping the annual cycle and reducing Fourier amplitude to be simply a measure of the annual mean. The second reason is that the Fourier-derived phase is of less inherent interest than the absolute length of the TC season, as measured by the time during which TCs are probable, however, that is precisely defined. So, while initially motivated by the effects of projected changes in the Fourier-derived seasonality of temperature, we will primarily focus on changes in the threshold-derived measures of seasonality for tropical cyclones, though we do still calculate their Fourier phases.

We calculate the threshold-derived seasonality of a variable by defining the start date of the season as the time when the variable crosses the threshold and is increasing, while the end date of the season occurs when

the variable crosses the threshold and is decreasing. We ignore data for which there are no crossings or more than two crossings (a start and an end), since they do not have well-defined annual cycles at that threshold value. We calculate the monthly climatology for each model and period of interest, which we then interpolate to daily using a cubic spline approach in order to better resolve the start and end dates. To determine the robustness of our results, we repeat our analysis using different thresholds.

We also calculate the length of the TC season by simply measuring the number of days between the first and last storms of the season. This works well in basins that only have TCs during a specific part of the year and less well in basins with TCs throughout the year because there is ambiguity about whether a storm is the first storm of the season, or the last one of the previous season. But in all basins it is useful as a complementary technique to the threshold analysis described above.

3. Climatology

Figure 2 shows the climatologies of tropical cyclones in different ocean basins for the observations, the downscaling method forced with output from the six CMIP5 models' historical simulations (D5), the downscaling model
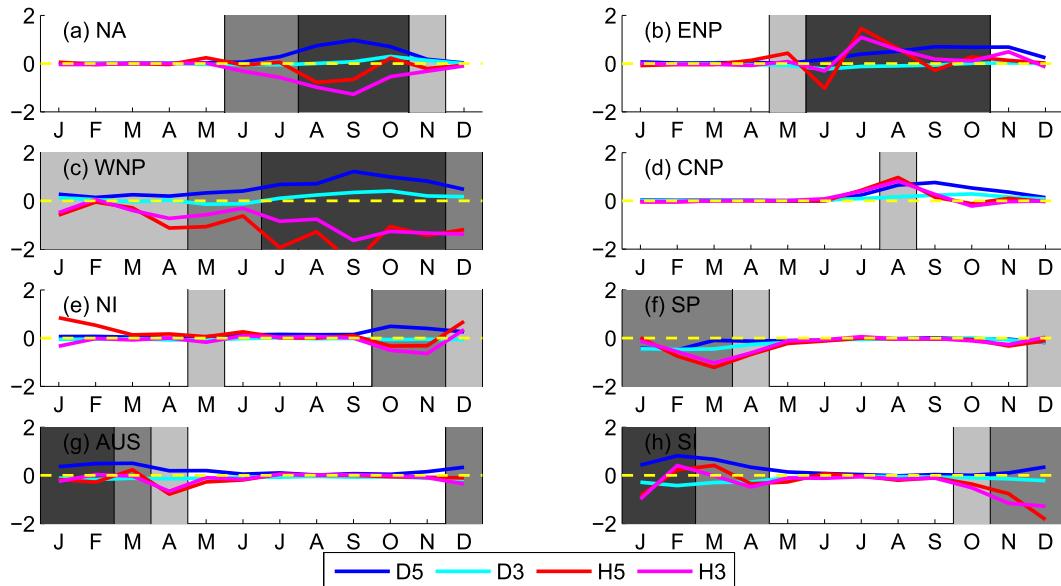
FIG. 3. Projected changes in the number of TCs in different ocean basins, as indicated by colored lines. Black shading shows months where the climatology has more than 2 TCs per month, medium gray shading is for between 1 and 2 TCs per month, and light gray shading is for between 0.5 and 1 TCs per month on average. The blue line shows the changes in D5, the downscaling model forced with CMIP5 data; the cyan line shows the changes for D3, the downscaling model forced with CMIP3 data; the red line shows the changes in H5, HiRAM forced with SST anomalies from CMIP5; and the magenta line shows the changes in H3, HiRAM forced with SST anomalies from CMIP3.

on the seven CMIP3 models' historical (20C3M) simulations (D3), and HiRAM forced with the observed climatological SST from the end of the twentieth century. First we focus on the observations, averaged over 1980–2012. In the North Atlantic, TCs commonly occur between June and November and most frequently between August and October. The eastern North Pacific has a similar distribution but with a broader peak shifted to earlier in the year and peaking between July and September. The western North Pacific is the most active basin globally with TCs occurring during all months of the year, though it maintains a strong annual cycle peaking between July and October. The central North Pacific is a relatively inactive basin, with no months averaging more than one tropical storm per month. The north Indian Ocean has a semiannual cycle with peaks in May and between October and December, with a quiescent period in between during monsoon season. In the Southern Hemisphere, the South Pacific, Australian basin, and south Indian Ocean have a similar climatology, with the highest frequency of TCs between January and March.

Figure 2 also includes the seasonal cycle of TCs from D5, D3, and HiRAM. All models capture the approximate seasonal cycle but are biased in some basins. For example, all models overestimate the frequency in the

central North Pacific and South Pacific, and they tend to peak around one month later than observations in the eastern North Pacific and Australian basins. In the most active basins, D5 produces fewer storms than observed, possibly because D5 (and D3) is run with model SST, while HiRAM is run with observed SST. For this reason, Fig. 2 does not present a fair evaluation of different model techniques, but rather shows that all sets of simulations considered in this study are able to capture the approximate timing and strength of the seasonal cycle of TCs.

4. Projected changes in the seasonal characteristics of tropical cyclones

Next we look at the projected changes and plot the change in the annual cycle of TC frequency for each basin in Fig. 3. In the North Atlantic and western North Pacific, two of the most active basins, there is an increase in storm frequency in D5, a small increase in D3, and decreases in both H5 and H3. In the eastern North Pacific, another very active basin, all ensembles except D3 project an increase in TC frequency. In some basins, such as the South Pacific, all models project a decrease in TC activity, while in other basins different models project differing overall frequency and timing changes. In
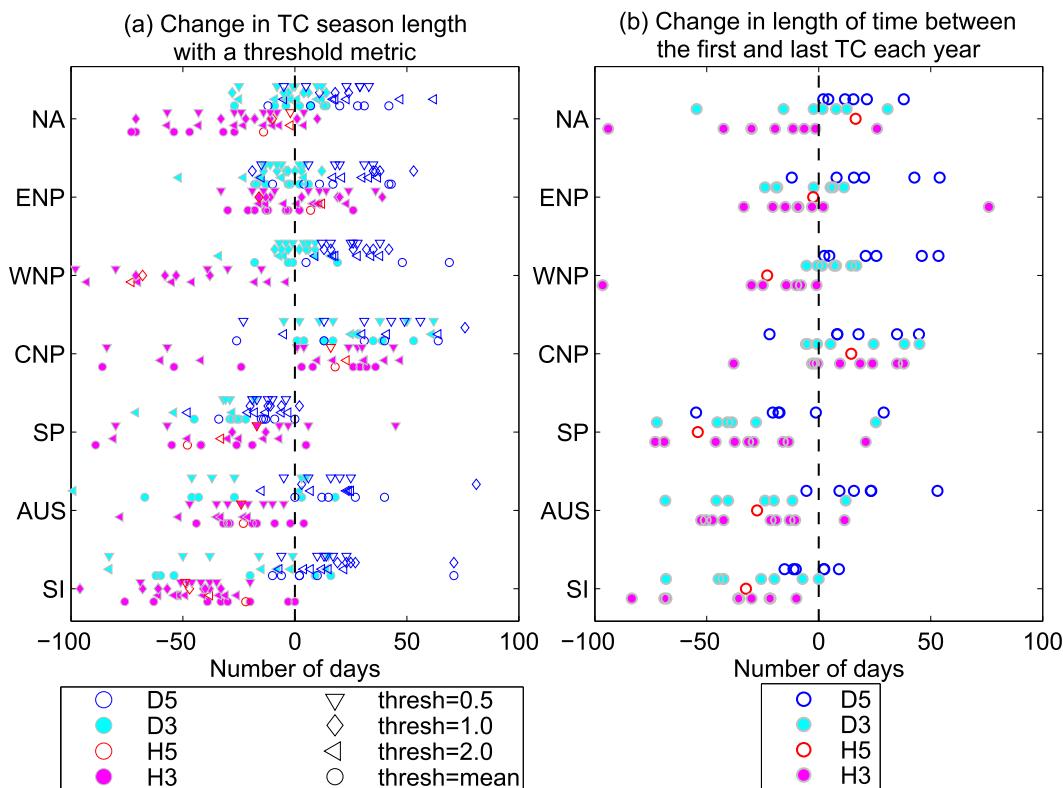
FIG. 4. Projected changes in the season length of the number of TCs as measured by (a) the number of days that the data are above a threshold and (b) the number of days between the first and last TC each year. In (a), we use thresholds of 0.5, 1, and 2 TCs per month, and the mean of the late twentieth-century TC frequency, which varies by model and basin.

the global picture, though, D5 projects an increase in TC frequency, D3 projects little change in storm frequency, while H5 and H3 project a decrease in storm frequency. These changes are largest during the peak season, indicated by the dark shading, but extend into the transition seasons too.

The larger changes in D5 relative to D3 must in some way be attributable to differences in the CMIP models, since the downscaling method has changed little between CMIP generations. There are many differences between CMIP5 and CMIP3 models. They have different greenhouse gas and aerosol emission scenarios, leading to different radiative forcing both at the top of the atmosphere and at the surface. CMIP5 models also have better resolution and different parameterizations compared to CMIP3. Moreover, the models included in D5 are not all merely later generations of the models in D3, but in some cases different models entirely, chosen because of data availability. And while H5 and H3 show similar changes, they both use the same observed SST for the twentieth century, whereas D5 and D3 use model output with different twentieth-century climatologies. These effects all may contribute to the relatively larger changes in D5.

As described in section 2, we use a threshold metric to determine the projected changes in TC season length. Since different threshold values will give quantitatively different answers for season length changes, we focus on 1) the qualitative changes and 2) what factors explain the changes in season length.

Figure 4a shows the changes in the length of the TC season as defined by the number of consecutive days that the tropical storm frequency (in units of TCs per month) is above thresholds of 0.5, 1.0, 2.0, and the mean TC frequency of the late twentieth century. The numerical values were chosen to capture season length across a range of models and basins (see Fig. 2), while the mean metric uses the average number of storms in the late twentieth century as a threshold and varies by model and basin. Any basin with TC frequency always above or below the threshold or exceeding the threshold in nonconsecutive months is ignored (e.g., we do not include the north Indian Ocean in Fig. 4a because of its very strong semiannual cycle). We present each available simulation but not the ensemble average, as different choices of CMIP scenarios and simulations do not enable direct comparison between each set of simulations.

Figure 4a shows that in most basins D5 projects a longer TC season, while D3 projects little change in most NH basins and a shorter season in the SH basins. H5 and H3 both project a shorter TC season in most basins, with some ensemble members shortening their season by as much as three months. While the quantitative changes depend on the threshold value and simulation, there is overall agreement on the sign of the changes with a few exceptions. In the eastern and central North Pacific, H3 and H5 do not project a shorter season. In the South Pacific, D5 projects a small reduction in season length, unlike in all of the other basins. Similar results are obtained when the season length changes were defined using the accumulated cyclone energy (Bell et al. 2000), rather than TC frequency (not shown).

We also studied the changes in TC season length for storms simulated directly in the CMIP5 models (also not shown). These models underestimate the mean global storm frequency but capture the seasonal behavior of TCs in most basins (Camargo 2013). In the western North Pacific, the only basin where nearly all CMIP5 models agree on the sign of the TC frequency change, the models project a much shorter season, similar to the behavior of H3 and H5 in that basin.

Another way to measure the length of the TC season is to calculate the length of time that passes between the first and last TC of a season. This measure works best in regions that have a stormy season and a quiescent season, but it can be applied in all basins. We define the year for Northern Hemisphere basins as 1 January–31 December and as 1 July–30 June for the Southern Hemisphere basins and find the first and last storms that happen during this period each year. Even in basins with a clear TC season, there is some ambiguity regarding whether a storm is being appropriately counted as the first of the season or the last of the previous season. We attempt to minimize the effect of these inappropriately counted storms by taking the median (rather than mean) date of the first and last storms.

We plot the changes in the length of the TC season as measured by the length of time between the first and last storm in Fig. 4b. The changes in season length echo those calculated by the threshold metric. D5 projects a longer season in most basins, including the three most active basins. D3 does not project a clear change in the NH basins, but does give a shorter season in the SH basins. H5 and H3 both project a shorter season in most basins. In most basins, different CMIP output can lead to season length changes of very different magnitudes, even in the same set of simulations. The clearest changes in TC season length are in the central North Pacific, with most models showing a longer season, consistent with other studies that have linked the increase in TC frequency to a northwestward shift of the eastern North Pacific TC tracks (Murakami et al. 2013) and the well-documented tendency of climate models to reduce the east–west gradients in SST and ocean heat content as the climate warms (DiNezio et al. 2009; Vecchi and Soden 2007).

Next we study whether changes in the TC season length are mainly due to a simple year-round multiplicative change in storm frequency or to the seasonal aspects of the change. We do this by first calculating two sets of idealized twenty-first-century TC climatologies, one with the twentieth-century annual cycle multiplied by a scaling factor $N'(t) = aN_{20}(t)$ and the other as the residual of this quantity $R(t) = N_{21}(t) + (1 - a)N_{20}(t)$, where $N(t)$ is the number of TCs each month, the subscripts refer to late twentieth- or twenty-first-century data, and a is the ratio of the annual mean twenty-first-century TC frequency to the annual mean twentieth-century TC frequency. The quantity $N'(t)$ has the shape of the twentieth-century TC climatology but the annual mean of the twenty-first-century TC climatology. The residual $R(t)$ captures changes in the shape (e.g., a peak that shifts or an extension into the inactive season), but its annual mean is that of the twentieth century. For both of these idealized quantities, calculated with a separate scaling factor for each model and basin, we determine the change in the length of the season relative to the twentieth-century value using the threshold method described in the previous section and compare it to the actual projected season length changes.

We start by plotting the actual change in season length against the change in season length when using $N'(t)$ as the twenty-first-century TC frequency time series in Fig. 5a. Correlating the changes in season length for each measure yields a positive correlation coefficient, to be expected since the year-round multiplicative change should positively contribute to season length changes when calculated with a threshold metric. The correlation coefficients are $r = 0.81$ for D5, $r = 0.93$ for D3, $r = 0.80$ for H5, and $r = 0.86$ for H3.

Perhaps more meaningful are the results of Fig. 5b, in which we plot the change in the actual season length against the change in the season length when using $R(t)$ as the twenty-first-century TC frequency time series. Here we also find a positive correlation, albeit smaller, with correlation coefficients of $r = 0.14$ for D5, $r = 0.14$ for D3, $r = 0.85$ for H5, and $r = 0.28$ for H3. Combining all models together yields $r = 0.24$ and a regression slope of 0.57, compared to $r = 0.89$ and a slope of 0.87 for the annual mean–like change. While smaller, a Student's t test reveals that the correlation is significantly different than zero at the 95% level, meaning that the year-round multiplicative change is not entirely responsible for the changes in season length. Instead there is contribution
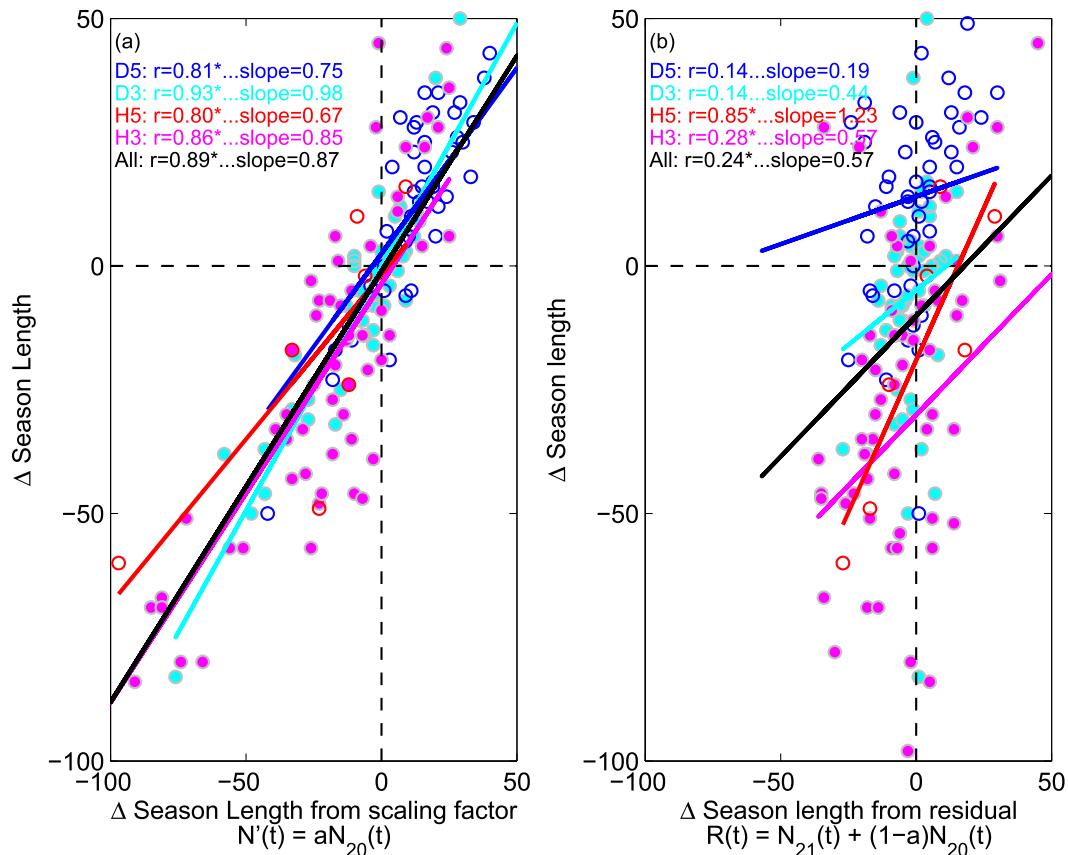
FIG. 5. Projected changes in the season length (days) of actual TC frequency (y axes) against season length changes from idealizations of the twenty-first-century TC frequency (x axes). We use (a) $N'(t)$ for the twenty-first century, which preserves the shape of the twentieth-century data, but it has the annual mean of the twenty-first-century data, and (b) the residual $R(t)$, which captures changes in the shape but maintains the annual mean of the twentieth century. Season length changes are calculated with the twentieth-century mean as a threshold. The correlation coefficients r and regression slopes are given in the figure for each model and for the combined model data. Asterisks after the correlation coefficients indicate statistical significance at the 95% level. These results suggest that most, but not all, of the change in season length is due to a year-round multiplicative factor change in storm frequency. Note that seven data points lie outside the axis bounds in both (a) and (b), but they are still included in the analysis.

from seasonal aspects of the changes in TC frequency. If more TCs occur in a given year, then they do not tend to be solely concentrated in the existing stormy months but also occur at the margins of the season, thus extending the season. Nonzero changes during the transition months can also be seen in Fig. 3.

Another metric often used to assess seasonality is the phase of the annual cycle, calculated via a Fourier transform. This metric cannot measure changes in season length, since the data are projected onto a sinusoid, but instead measures the timing of the annual cycle relative to the calendar year. Because it does not depend on the annual mean value of the data, it offers an independent objective measure of seasonality. Using this metric previous work has found the CMIP3 and CMIP5 models project a delay in the annual cycles of SST,

precipitation, and the circulation in the tropics, indicating a shift in the extrema of these quantities to later in the year. Does this also occur for TCs?

Figure 6 shows the change in the phase of the annual cycle of TCs only for simulations with a strong annual cycle (i.e., the annual cycle for both the twentieth- and twenty-first-century simulations makes up at least 60% of the total variance). The phase changes vary considerably by basin and model. In the North Atlantic, nearly all of the D5 models and most of the D3 and H3 models project a phase delay. In the eastern North Pacific, the majority of models also project a phase delay, while in the western North Pacific, nearly all of the H3 models project a phase advance (shift to earlier) and the D3 models almost all project a phase delay. In the south Indian Ocean, most models project a phase delay,
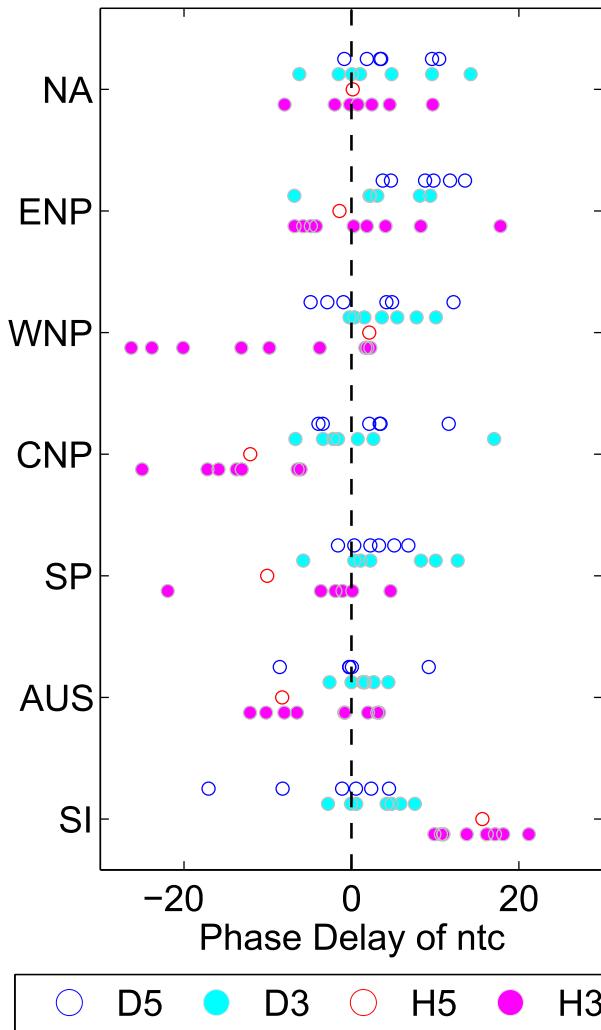
FIG. 6. Projected changes in the phase of the annual cycle of TC frequency. Phase is calculated via Fourier transform and ignores any changes in the annual mean. Positive values indicate a phase delay, or shift of TCs to later in the calendar year. For each basin we only plot models for which the annual cycle captures at least 60% of the total variance.

especially for H5 and H3. While CMIP3 and CMIP5 models mostly project a phase delay in SST and other aspects of tropical climate, these do not translate to a phase delay in the number of storms according to the downscaling and HiRAM models.

5. Projected changes in the seasonal characteristics of a tropical cyclone genesis index

To gain a better understanding of the nature of the seasonal changes in TC frequency, we look at the changes in a tropical cyclone genesis index (TCGI; Tippett et al. 2011), which relates TC activity to environmental fields. The index we use was developed by
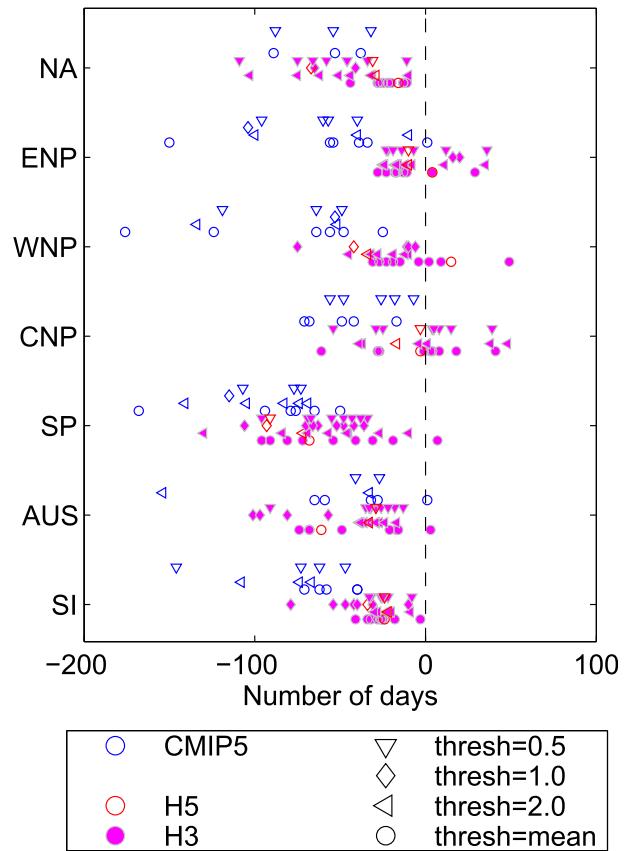
FIG. 7. As in Fig. 4a, but for the change in the season length of the TCGI.

Camargo et al. (2014) following the technique of Tippett et al. (2011) and uses clipped absolute vorticity, vertical wind shear, saturation deficit, and potential intensity (Bister and Emanuel 2002) to model tropical cyclone genesis. Using HiRAM, Camargo et al. (2014) determined coefficients that form the optimal combination of these variables for describing TC activity in HiRAM in both the present and future climates. Here we apply a similar index for the CMIP5 models used by the downscaling method. Because the CMIP5 models do not directly simulate TCs adequately because of coarse resolution and other factors (Camargo 2013), the TCGI coefficients used for the CMIP5 models are derived from a reanalysis, ERA-Interim (Dee and Uppala 2009), and observed TC data and then calculated for each CMIP5 model using the environmental fields from present and future climates.

Figure 7 shows the projected changes in the season length of basin-integrated TCGI for CMIP5, H5, and H3, calculated in the same way as for the changes in TC season length. (We did not calculate the TCGI for CMIP3 because of time constraints.) There is a shorter

season for each set of simulation in most basins, including the North Atlantic, western North Pacific, and the SH basins. For H3 and H5, some ensemble members give a longer season or no change of TCGI in the eastern and central North Pacific, but elsewhere the projection of a shorter TCGI season is very robust. The decreases are especially dramatic for CMIP5: only two ensemble members in any basin do not project a shorter season. Some of the decreases were so large that they were not plotted, since the twenty-first-century data did not meet even the smallest threshold.

The shorter season in TCGI for H3 and H5 are in agreement with a shorter season in TC frequency (Fig. 4a), both in the global mean and on a basin-by-basin level. However, the much shorter season in TCGI for CMIP5 is in contrast to D5's projections of a longer season in many basins. It is not fully clear why this is the case. Most genesis indices, like the one used in Emanuel (2013), project an increase in future global TC frequency. But these indices disagree with most models' projections of decreasing TC frequency (Knutson et al. 2010). Our choice of genesis index captures not only present-day TC frequency but also future TC frequency, as projected by a large number of models. Ultimately, resolving this issue is beyond the scope of the present work.

6. Summary

We study projected changes in the length of the tropical cyclone season for the end of the twenty-first century compared to the end of the twentieth century using two sets of simulations that are able to capture the approximate timing of the tropical cyclone season. These datasets, from a downscaling method applied to both CMIP5 and CMIP3 data (D5 and D3) and from HiRAM, an AGCM forced with both CMIP5 and CMIP3 SST anomalies (H5 and H3), give different projections for the changes in the season length of the TC season. When calculated using a threshold measure, D5 projects longer seasons in most basins, D3 projects a slight decrease in season length, and H5 and H3 project shorter seasons in most basins. In the central North Pacific, most models agree on a longer season, while in the South Pacific, most models project a shorter season. Projections in other basins vary by model. These changes are robust to the method used to define season length; different threshold values and a measure in which season length is defined as the length of time between the first and last TC each year give the same qualitative results.

We also find that the twenty-first-century changes in season length are not entirely due to mean changes. By idealizing the projected twenty-first-century annual

cycle of TC frequency as a component that preserves the shape of the twentieth-century climatology but alters the annual mean and a residual component that does the opposite, we find that while the year-round multiplicative change explains a large amount of the change in season length, the residual component also contributes to the changes. This suggests that the observed trend toward a longer TC season in the North Atlantic (Kossin 2008) is mainly a result of an increasing frequency of TCs over the past few decades in that basin.

When using a Fourier measure of seasonality for the number of storms (which does not allow for changes in season length), the results vary by model and basin. In the North Atlantic, most models project a timing shift to later in the year, while in the western North Pacific, H3 projects a large shift to earlier in the year, and in the eastern North Pacific there is some indications of a shift to later in the year. In the other basins, the results vary by model. Finally, we look at the projected changes in season length for a genesis index for tropical cyclones. Season length changes for that environmental index agree with those for storm frequency for H3 and H5, adding confidence to these findings, while D5 models do not show the same agreement. Ultimately, there is not yet a consensus on how the length of the TC season will change as a result of anthropogenic effects.

REFERENCES

Bell, G. D., and Coauthors, 2000: Climate assessment for 1999. *Bull. Amer. Meteor. Soc.,* **81,** S1–S50, doi:10.1175/1520-0477(2000)81[s1:CAF]2.0.CO;2.

Bengtsson, L., K. I. Hodges, M. Esch, N. Keenlyside, L. Kornblueh, J.-J. Luo, and T. Yamagata, 2007: How may tropical cyclones change in a warmer climate? *Tellus,* **59A,** 539–561, doi:10.1111/j.1600-0870.2007.00251.x.

Biasutti, M., and A. Sobel, 2009: Delayed Sahel rainfall and global seasonal cycle in a warmer climate. *Geophys. Res. Lett.,* **36,** L23707, doi:10.1029/2009GL041303.

Bister, M., and K. A. Emanuel, 2002: Low frequency variability of tropical cyclone potential intensity 1. Interannual to interdecadal variability. *J. Geophys. Res.,* **107,** 4801, doi:10.1029/2001JD000776.

Camargo, S. J., 2013: Global and regional aspects of tropical cyclone activity in the CMIP5 models. *J. Climate,* **26,** 9880–9902, doi:10.1175/JCLI-D-12-00549.1.

——, M. K. Tippett, A. H. Sobel, G. A. Vecchi, and M. Zhao, 2014: Testing the performance of tropical cyclone genesis indices in future climates using the HiRAM model. *J. Climate,* **27,** 9171–9196, doi:10.1175/JCLI-D-13-00505.1.

Chou, C., J.-Y. Tu, and P.-H. Tan, 2007: Asymmetry of tropical precipitation change under global warming. *Geophys. Res. Lett.,* **34,** L17708, doi:10.1029/2007GL030327.

Chu, J. H., C. R. Sampson, A. S. Levine, and E. Fukada, 2002: The Joint Typhoon Warning Center tropical cyclone best-tracks, 1945-2000. Naval Research Laboratory Tech. Rep. NRL/MR/7540-02-16, 22 pp.

Dee, D., and S. Uppala, 2009: Variational bias correction of satellite radiance data in the ERA-Interim reanalysis. *Quart. J. Roy. Meteor. Soc.,* **135,** 1830–1841, doi:10.1002/qj.493.

DiNezio, P. N., A. C. Clement, G. A. Vecchi, B. J. Soden, B. P. Kirtman, and S.-K. Lee, 2009: Climate response of the equatorial Pacific to global warming. *J. Climate,* **22,** 4873–4892, doi:10.1175/2009JCLI2982.1.

Dwyer, J. G., M. Biasutti, and A. H. Sobel, 2012: Projected changes in the seasonal cycle of surface temperature. *J. Climate,* **25,** 6359–6374, doi:10.1175/JCLI-D-11-00741.1.

——, ——, and ——, 2014: The effect of greenhouse gas–induced changes in SST on the annual cycle of zonal mean tropical precipitation. *J. Climate,* **27,** 4544–4565, doi:10.1175/JCLI-D-13-00216.1.

Emanuel, K. A., 2013: Downscaling CMIP5 climate models shows increased tropical cyclone activity over the 21st century. *Proc. Natl. Acad. Sci. USA,* **110,** 12 219–12 224, doi:10.1073/pnas.1301293110.

——, C. DesAutels, C. Holloway, and R. Korty, 2004: Environmental control of tropical cyclone intensity. *J. Atmos. Sci.,* **61,** 843–858, doi:10.1175/1520-0469(2004)061<0843:ECOTCI>2.0.CO;2.

——, S. Ravela, E. Vivant, and C. Risi, 2006: A statistical deterministic approach to hurricane risk assessment. *Bull. Amer. Meteor. Soc.,* **87,** 299–314, doi:10.1175/BAMS-87-3-299.

——, R. Sundararajan, and J. Williams, 2008: Hurricanes and global warming: Results from downscaling IPCC AR4 simulations. *Bull. Amer. Meteor. Soc.,* **89,** 347–367, doi:10.1175/BAMS-89-3-347.

Held, I. M., and M. Zhao, 2011: The response of tropical cyclone statistics to an increase in CO_2 with fixed sea surface temperatures. *J. Climate,* **24,** 5353–5364, doi:10.1175/JCLI-D-11-00050.1.

Huang, P., S.-P. Xie, K. Hu, G. Huang, and R. Huang, 2013: Patterns of the seasonal response of tropical rainfall to global warming. *Nat. Geosci.,* **6,** 357–361, doi:10.1038/ngeo1792.

JTWC, 2015: Joint Typhoon Warning Center tropical cyclone best track data site. [Available online at http://www.usno.navy.mil/NOOC/nmfc-ph/RSS/jtwc/best_tracks/.]

Knutson, T. R., J. J. Sirutis, S. T. Garner, G. A. Vecchi, and I. M. Held, 2008: Simulated reduction in Atlantic hurricane frequency under twenty-first-century warming conditions. *Nat. Geosci.,* **1,** 359–364, doi:10.1038/ngeo202.

——, and Coauthors, 2010: Tropical cyclones and climate change. *Nat. Geosci.,* **3,** 157–163, doi:10.1038/ngeo779.

——, and Coauthors, 2013: Dynamical downscaling projections of twenty-first-century Atlantic hurricane activity: CMIP3 and CMIP5 model-based scenarios. *J. Climate,* **26,** 6591–6617, doi:10.1175/JCLI-D-12-00539.1.

Korty, R. L., S. J. Camargo, and J. Galewsky, 2012: Variations in tropical cyclone genesis factors in simulations of the Holocene epoch. *J. Climate,* **25,** 8196–8211, doi:10.1175/JCLI-D-12-00033.1.

Kossin, J. P., 2008: Is the North Atlantic hurricane season getting longer? *Geophys. Res. Lett.,* **35,** L23705, doi:10.1029/2008GL036012.

Landsea, C. W., and J. L. Franklin, 2013: Atlantic hurricane database uncertainty and presentation of a new database format. *Mon. Wea. Rev.,* **141,** 3576–3592, doi:10.1175/MWR-D-12-00254.1.

Meehl, G. A., C. Covey, K. E. Taylor, T. Delworth, R. J. Stouffer, M. Latif, B. McAvaney, and J. F. B. Mitchell, 2007: The WCRP CMIP3 multimodel dataset: A new era in climate change research. *Bull. Amer. Meteor. Soc.,* **88,** 1383–1394, doi:10.1175/BAMS-88-9-1383.

Murakami, H., B. Wang, T. Li, and A. Kitoh, 2013: Projected increase in tropical cyclones near Hawaii. *Nat. Climate Change,* **3,** 749–754, doi:10.1038/nclimate1890.

——, P.-C. Hsu, O. Arakawa, and T. Li, 2014: Influence of model biases on projected future changes in tropical cyclone frequency of occurrence. *J. Climate,* **27,** 2159–2181, doi:10.1175/JCLI-D-13-00436.1.

NHC, 2015: National Hurricane Center best track data. [Available online at http://www.nhc.noaa.gov/data/#hurdat.]

Schreck, C. J., III, K. R. Knapp, and J. P. Kossin, 2014: The impact of best track discrepancies on global tropical cyclone climatologies using IBTrACS. *Mon. Wea. Rev.,* **142,** 3881–3899, doi:10.1175/MWR-D-14-00021.1.

Seth, A., S. A. Rauscher, M. Biasutti, A. Giannini, S. J. Camargo, and M. Rojas, 2013: CMIP5 projected changes in the annual cycle of precipitation in monsoon regions. *J. Climate,* **26,** 7328–7351, doi:10.1175/JCLI-D-12-00726.1.

Sobel, A., and S. Camargo, 2011: Projected future seasonal changes in tropical summer climate. *J. Climate,* **24,** 473–487, doi:10.1175/2010JCLI3748.1.

Sugi, M., A. Noda, and N. Sato, 2002: Influence of the global warming on tropical cyclone climatology: An experiment with the JMA global model. *J. Meteor. Soc. Japan,* **80,** 249–272.

Taylor, K. E., R. J. Stouffer, and G. A. Meehl, 2012: An overview of CMIP5 and the experiment design. *Bull. Amer. Meteor. Soc.,* **93,** 485–498, doi:10.1175/BAMS-D-11-00094.1.

Tippett, M. K., S. J. Camargo, and A. H. Sobel, 2011: A Poisson regression index for tropical cyclone genesis and the role of large-scale vorticity in genesis. *J. Climate,* **24,** 2335–2357, doi:10.1175/2010JCLI3811.1.

Tory, K. J., S. S. Chand, R. A. Dare, and J. L. McBride, 2013: An assessment of a model-, grid-, and basin-independent tropical cyclone detection scheme in selected CMIP3 global climate models. *J. Climate,* **26,** 5508–5522, doi:10.1175/JCLI-D-12-00511.1.

Vecchi, G. A., and B. J. Soden, 2007: Global warming and the weakening of the tropical circulation. *J. Climate,* **20,** 4316–4340, doi:10.1175/JCLI4258.1.

Villarini, G., and G. A. Vecchi, 2012: Twenty-first-century projections of North Atlantic tropical storms from CMIP5

models. *Nat. Climate Change,* **2,** 604–607, doi:10.1038/nclimate1530.

——, and ——, 2013: Projected increases in North Atlantic tropical cyclone intensity from CMIP5 models. *J. Climate,* **26,** 3231–3240, doi:10.1175/JCLI-D-12-00441.1.

Wu, L., and Coauthors, 2014: Simulations of the present and late-twenty-first-century western North Pacific tropical cyclone activity using a regional model. *J. Climate,* **27,** 3405–3424, doi:10.1175/JCLI-D-12-00830.1.

Yan, Y., Y. Qi, and W. Zhou, 2012: Variability of tropical cyclone occurrence date in the South China Sea and its relationship with SST warming. *Dyn. Atmos. Oceans,* **55–56,** 45–59, doi:10.1016/j.dynatmoce.2012.05.001.

Zhao, M., and I. M. Held, 2012: TC-permitting GCM simulations of hurricane frequency response to sea surface temperature anomalies projected for the late-twenty-first century. *J. Climate,* **25,** 2995–3009, doi:10.1175/JCLI-D-11-00313.1.

——, ——, S.-J. Lin, and G. A. Vecchi, 2009: Simulations of global hurricane climatology, interannual variability, and response to global warming using a 50-km resolution GCM. *J. Climate,* **22,** 6653–6678, doi:10.1175/2009JCLI3049.1.